International Journal of Mechanical, Industrial and Aerospace Sciences
ISSN: 2517-9950
Vol:5, No:11, 2011

Target Trajectory Design of Parametrically Excited Inverted Pendulum for Efficient Bipedal Walking

Toyoyuki Honjo, Takeshi Hayashi, Akinori Nagano and Zhi-Wei Luo

Abstract—For stable bipedal gait generation on the level floor, efficient restoring of mechanical energy lost by heel collision at the ground is necessary. Parametric excitation principle is one of the solutions. We dealt with the robot's total center of mass as an inverted pendulum to consider the total dynamics of the robot. Parametrically excited walking requires the use of continuous target trajectory that is close to discontinuous optimal trajectory. In this paper, we proposed the new target trajectory based on a position in the walking direction. We surveyed relations between walking performance and the parameters that form the target trajectory via numerical simulations. As a result, it was found that our target trajectory has the similar characteristics of a parametrically excited inverted pendulum.

Keywords—Dynamic Bipedal Walking, Parametric Excitation, Target Trajectory Design.

I. Introduction

EFFICIENT walking strategies have been studied in the field of bipedal locomotion. As one of the most energy-efficient walking approaches, passive dynamic walking has been proposed by McGeer [1]. In passive dynamic walking, a biped robot continuously and stably walks down a gentle slope without any actuators or mechanical inputs when the robot is placed on a suitable initial condition. The loss of mechanical energy is caused by the collision between the edge of swing-leg and the walking surface. In this walking approach, mechanical energy is restored by transporting potential energy to kinetic energy while descending the slope. However, bipedal walking on the level floor has no propulsion generated by gravity and can not transport potential energy to kinetic energy. Therefore, mechanical energy must be restored through some mechanical inputs to realize bipedal walking on the level floor. Goswami et al. proposed energy tracking control in which the hip and ankle torque were designed to make the energy level constant in a sustainable gait and showed that the energy tracking control made a stable limit cycle [2]. Asano et al. proposed a so-called virtual passive dynamic walking [3]. The hip and ankle torque were designed based on virtual gravity. Asano et al. also applied virtual passive dynamic walking approach to a biped robot with semicircular feet whose center is located on the legs [4]-[5]. They have shown that the rolling of semicircular feet has an effect similar to ankle torque. Hence, the robot can restore the energy dissipated at the impact by using only hip torque and generate a sustainable gait.

One of other approaches for restoring mechanical energy is parametric excitation. Asano et al. applied a parametric excitation principle to a biped robot with telescopical actuator in its legs to change the position of the leg's mass center [6]-[8]. Harata et al. proposed to apply parametric excitation to a biped robot with knee joint and semicircular feet [9]-[11]. They showed that bending and extending the knee have an effect similar to telescopic-leg and the robot generated a sustainable gait. We proposed parametrically excited walking of an inverted pendulum to consider the dynamics of support-leg [12]. We dealt with the robot's total center of mass as an inverted pendulum and controlled the trajectory of mass center to be closer to optimal trajectory of a parametrically excited inverted pendulum. For efficient parametrically excited walking, Banno et al. and Harata et al. applied a target trajectory that was represented by a combination of spline functions to a bipedal robot [13]-[14]. In these methods, target trajectories were designed as a time function. However, the dynamics of gait is complex and it is hard to predict the behavior of stable dynamical gait. Therefore, it is difficult to actuate the knee joint or telescopical mechanics at the arbitrary timing.

For efficient bipedal walking, the target trajectory as a function of spatial coordinates is required to actuate the knee joint or telescopical mechanics at the arbitrary timing. Therefore, we proposed a new target trajectory based on a position relative to the walking direction. This target trajectory was represented by a product of two sigmoid functions. This method requires no information of the walking behavior to set parameters of the target trajectory. The proposed trajectory enables the robot to actuate the knee joint of its swing-leg at the desired timing even if the walking speed or walking stride changes. In this paper, we examined the relationships between the performance of the system and the effect of parameters that determine the shape of the target trajectory via numerical walking simulations. As a result, we found that there is an optimal parameter set for efficient parametrically excited walking with knee joint actuation.

This paper is organized as follows: Section II explains the planar kneed biped robot with semicircular feet. Section III explains the parametric excitation of an inverted pendulum and verifies the effects of the proposed trajectory via numerical simulations. Section IV verifies the performance of the proposed parametrically excited walking via numerical walking simulations and shows those simulation results. Finally, Section V gives our conclusion.

T. Honjo is with the Graduate School of Engineering, Kobe University, 1-1 Rokkodai-cho, Nada, Kobe, Hyogo, 657-8501 JAPAN (e-mail: carcharomack@cs11.cs.kobe-u.ac.jp).

T. Hayashi is with the Human Technology Research Institute, National Institute of Advanced Industrial Science and Technology.

A. Nagano and Z.W. Luo are with the Graduate School of System Informatics, Kobe University.

II. Planar kneed biped robot

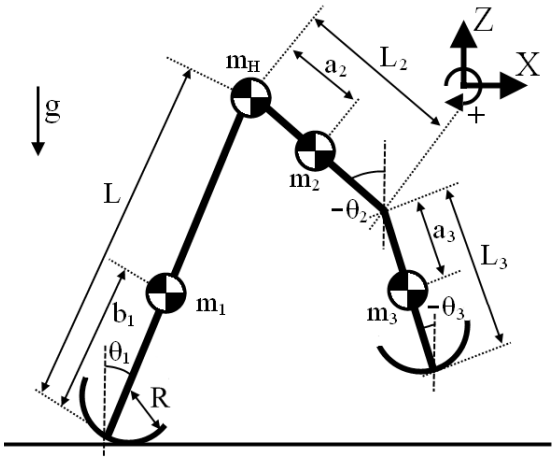

Fig. 1. Model of a planar kneed biped robot with semicircular feet

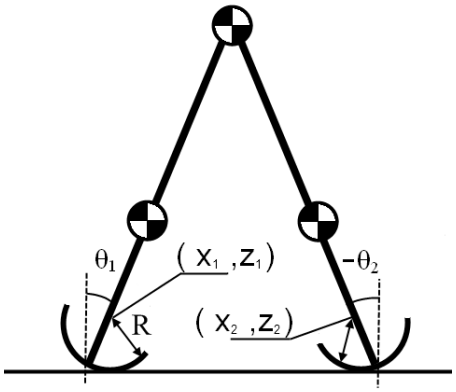

Fig. 2. Configuration at the instant of the double support phase

The biped robot used in this paper is illustrated in Fig. 1. This robot has the knee joint and semicircular feet whose center is located on the leg. Dynamic biped walking of this robot consists of two phases. One phase is the single support phase and another phase is the double support phase. In the single support phase, the support-leg constantly contacts the walking surface and rotates around the contact point. The knee joint of the support-leg is locked in a straight posture by mechanical constraint. The swing-leg swings and only the knee joint of the swing-leg is controlled based on our target trajectory. After bending and stretching the knee joint of the swing-leg, the knee joint of the swing-leg is also locked in a straight posture by mechanical constraint. Therefore, this robot has two or three degrees of freedom during the single support phase. The lock of the swing-leg's knee occurs before the heel of the swing-leg strikes the ground. The single support phase shifts to the double support phase when a collision occurs at the ground.

The double support phase is an instantaneous event. During the double support phase, the support-leg and the swing-leg are exchanged and the knee joint of the new swing-leg becomes free. After updating the states, the double support phase shifts to the single support phase and the next step is generated.

The dynamic equation during the single support phase is given by

$$\boldsymbol{M}(\boldsymbol{\theta})\ddot{\boldsymbol{\theta}} + \boldsymbol{h}(\boldsymbol{\theta}, \dot{\boldsymbol{\theta}}) = \boldsymbol{S}\boldsymbol{u}_K - \boldsymbol{J}_K^{\mathrm{T}}\lambda_K,$$

where $\boldsymbol{\theta} = [\theta_1\ \theta_2\ \theta_3]^{\mathrm{T}}$ is the generalized coordinate vector, $\boldsymbol{M}$ is the inertia matrix, $\boldsymbol{h}$ is the vector in which the Coriolis force, centrifugal force and gravity term are included. $\boldsymbol{J}_K = [0\ 1\ -1]$ is the Jacobian vector and $\lambda_K \in \mathbb{R}$ is the binding force that keeps the straight posture of the knee joint. $\boldsymbol{S}\boldsymbol{u}_K$ is the knee torque and the detail is explained later.

When the mechanical constraint of the knee joint occurs and the sole contacts the ground, a completely inelastic collision is assumed to occur at the knee of the swing-leg and the ground contact points, respectively. The transition of the angular velocities occurs between before and after the knee constraint or between before and after the ground contact. Angler velocities before and after the knee constraint are represented as $\dot{\boldsymbol{\theta}}^-$ and $\dot{\boldsymbol{\theta}}^+$. The transition of the angular velocities is given by

$$\boldsymbol{M}(\boldsymbol{\theta})\dot{\boldsymbol{\theta}}^+ = \boldsymbol{M}(\boldsymbol{\theta})\dot{\boldsymbol{\theta}}^- + \boldsymbol{J}_K^{\mathrm{T}}\lambda_K,$$

where λ_K is a constraint force that makes $\dot{\theta}_2^+ = \dot{\theta}_3^+$. This force is given by

$$\lambda_K = -\left(\boldsymbol{J}_K\boldsymbol{M}^{-1}(\boldsymbol{\theta})\boldsymbol{J}_K^{\mathrm{T}}\right)^{-1}\boldsymbol{J}_K\dot{\boldsymbol{\theta}}^-. \tag{1}$$

From this force, angular velocities after the knee constraint are given by

$$\dot{\boldsymbol{\theta}}^+ = \left(\boldsymbol{I} - \boldsymbol{M}^{-1}(\boldsymbol{\theta})\boldsymbol{J}_K^{\mathrm{T}}\left(\boldsymbol{J}_K\boldsymbol{M}^{-1}(\boldsymbol{\theta})\boldsymbol{J}_K^{\mathrm{T}}\right)^{-1}\boldsymbol{J}_K\right)\dot{\boldsymbol{\theta}}^-. \tag{2}$$

To describe the state transition at the double support phase, we define generalized coordinates $\boldsymbol{q} \in \mathbb{R}^6 = [x_1\ z_1\ \theta_1\ x_2\ z_2\ \theta_2]^{\mathrm{T}}$. As shown in Fig.2, $(x_i, z_i)\ (i = 1, 2)$ are located on the center of the support-leg's and swing-leg's semicircular feet, respectively. The transition between before and after the ground impact is given by

$$\boldsymbol{M}(\boldsymbol{q})\dot{\boldsymbol{q}}^+ = \boldsymbol{M}(\boldsymbol{q})\dot{\boldsymbol{q}}^- + \boldsymbol{J}_G^{\mathrm{T}}\lambda_G,$$

where $\dot{\boldsymbol{q}}^-$ and $\dot{\boldsymbol{q}}^+$ are velocities before and after the ground impact. $\boldsymbol{J}_G^{\mathrm{T}}$ is a Jacobian matrix that satisfies $\boldsymbol{J}_G\dot{\boldsymbol{q}}^+ = 0$ and λ_G is an undetermined multiplier vector that represents the impulse force. Velocities after the ground impact are given by

$$\dot{\boldsymbol{q}}^+ = \left(\boldsymbol{I} - \boldsymbol{M}^{-1}(\boldsymbol{q})\boldsymbol{J}_G^{\mathrm{T}}\left(\boldsymbol{J}_G\boldsymbol{M}^{-1}(\boldsymbol{q})\boldsymbol{J}_G^{\mathrm{T}}\right)^{-1}\boldsymbol{J}_G\right)\dot{\boldsymbol{q}}^-. \tag{3}$$

In addition, the support-leg and swing-leg are exchanged each other.

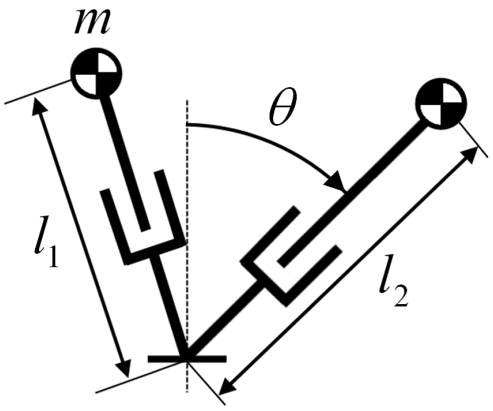

Fig. 3. Model of an inverted pendulum

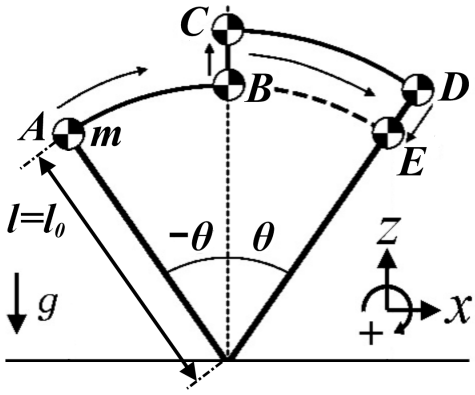

Fig. 4. Optimal trajectory of a parametrically excited inverted pendulum

III. Parametric excitation of an inverted pendulum

In this section, firstly we explain the parametric excitation of an inverted pendulum and our target trajectory. Then, we verify the relationships between the performance of an inverted pendulum and the effect of parameters of proposed target trajectory via numerical simulations.

A. Optimal trajectory of a parametrically excited inverted pendulum

The simple example of parametric excitation is a swing at a park. When we play on a swing, we bend and stretch our knee to increase the amplitude of the swing. In this situation, we control the position of mass center using our knee.

In some walking approaches, parametric excitation principle has been applied to the swing-leg of a biped robot [6]-[14]. We dealt with the dynamics of the biped robot as an inverted pendulum to consider the effect of the support-leg and proposed the parametric excitation of an inverted pendulum [12]. Fig. 3 shows the inverted pendulum that we dealt with in this paper. The optimal trajectory of a parametrically excited inverted pendulum shows Fig. 4. This optimal trajectory is derived by following equations:

$$\begin{aligned} K &= \tfrac{1}{2}ml^2\dot{\theta}^2 \\ L &= ml^2\dot{\theta} \\ \dot{L} &= mgl\sin\theta \end{aligned} \tag{4}$$

where K is kinetic energy, L is angular momentum, m, l are the mass and length of an inverted pendulum, g is gravity acceleration and θ is the angle of an inverted pendulum which has positive value when the angle is clockwise from vertical line. It is assumed that the length of pendulum l can be changed instantaneously. However, in reality, the length can not be changed instantaneously. Therefore, continuous target

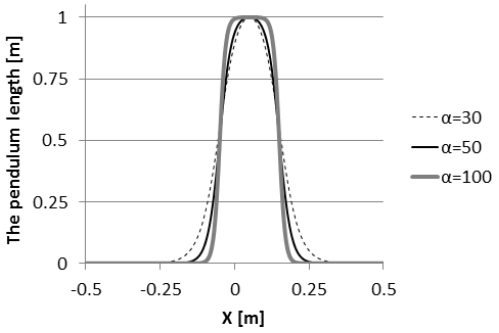

Fig. 5. Target trajectories at three values of α when $\beta_1 = -0.05$ and $\beta_2 = 0.15$

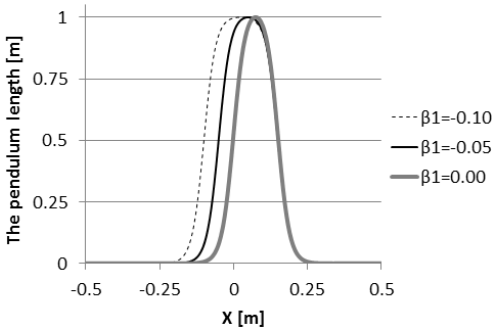

Fig. 6. Target trajectories at three values of β_1 when $\alpha = 50$ and $\beta_2 = 0.15$

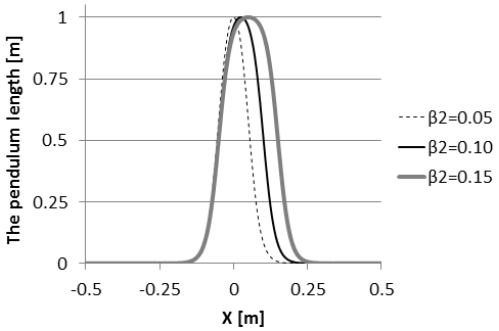

Fig. 7. Target trajectories at three values of β_2 when $\alpha = 50$ and $\beta_1 = -0.05$

trajectories that is close to the discontinuous optimal trajectory have been studied. In this paper, we proposed the target trajectory based on a position in the locomotive direction. Proposed target trajectory is represented by a product of two sigmoid functions and described as the following form:

$$l_d(x) = l_0 + \frac{A}{1+e^{-\alpha(x-\beta_1)}} \times \frac{1}{1+e^{\alpha(x-\beta_2)}} \tag{5}$$

$$\dot{l}_d(x) = \frac{\alpha A \dot{x}\left(e^{-\alpha(x-\beta_1)} - e^{\alpha(x-\beta_2)}\right)}{\left[1+e^{\alpha(\beta_1-\beta_2)}+e^{-\alpha(x-\beta_1)}+e^{\alpha(x-\beta_2)}\right]^2} \tag{6}$$

where l_0 is the initial length of the pendulum, A, α, β_1 and β_2 are parameters that determine the shape of target trajectory. A is the amplitude of trajectory, α is the magnitude of lift and descent pace, β_1 and β_2 are positions of lift and descent. From eq.(6), this trajectory has the maximum value when x is $\frac{\beta_1+\beta_2}{2}$. However, when α is small or the interval from β_1 to β_2 is short, this maximum value of eq.(5) is smaller than A. Therefore, we introduced the new amplitude $\hat{A}$ to normalize this function.

$$\hat{A} = A\left(1+2e^{\alpha\frac{(\beta_1-\beta_2)}{2}}+e^{\alpha(\beta_1-\beta_2)}\right) \tag{7}$$

The target trajectory is rewritten as

$$l_d(x) = l_0 + \frac{\hat{A}}{1+e^{-\alpha(x-\beta_1)}} \times \frac{1}{1+e^{\alpha(x-\beta_2)}}. \tag{8}$$

Several examples of our target trajectory are illustrated in Fig. 5-7.

When α is larger, this target trajectory gets closer to the optimal trajectory. However, larger α may decrease the stability or efficiency. Therefore, we verified the relation between the effect of these parameters and performances of the system.

B. Simulations of an inverted pendulum

We controlled an inverted pendulum that was illustrated in Fig. 3 to verify the validity of our proposed target trajectory. Dynamic equation of the inverted pendulum is described as the following form:

$$\boldsymbol{M}(\boldsymbol{q})\ddot{\boldsymbol{q}} + \boldsymbol{h}(\boldsymbol{q},\dot{\boldsymbol{q}}) = \boldsymbol{S}\boldsymbol{u}, \tag{9}$$

where $\boldsymbol{M} \in \mathbb{R}^{2\times2}$ is the inertia matrix, $\boldsymbol{h} \in \mathbb{R}^2$ is the vector in which the Coriolis force, centrifugal force and gravity term are included, $\boldsymbol{q} = [l\ \theta]^{\mathrm{T}}$ is the generalized coordinate vector, $\boldsymbol{S}u \in \mathbb{R}^2 = [1\ 0]^{\mathrm{T}}u$ is the control input vector. The initial condition is given by $\boldsymbol{q}_0 = [l_0\ \theta_0]^{\mathrm{T}}\ \ (\theta_0 < 0)$ and the termination condition is given by $\boldsymbol{q}_T = [l_T\ \theta_T]^{\mathrm{T}}\ \ (l_T = l_0, \theta_T = |\theta_0|)$.

We evaluate the performance of the system using two performance indicators. One is the increment of mechanical energy $\Delta E = E_T - E_0$. Another is the specific resistance μ. The specific resistance is the indicator of locomotive energy efficiency. The specific resistance μ is defined by

$$\mu = \frac{\int_{0+}^{T^-}\left(\left|\dot{l}u\right|\right)\mathrm{d}t.}{M_g g \Delta X_g}, \tag{10}$$

where T^- is the step time, M_g is the total mass of the system, g is the gravity acceleration and ΔX_g is the moving distance of mass center during one step. Numerator of eq. (10) shows the actuator's work and the specific resistance μ shows the amount of energy that the system requires to move unit distance when the mass of the system is unit weight. Therefore, the locomotive system is efficient when μ is small. Physical parameters of this inverted pendulum are listed in Table I.

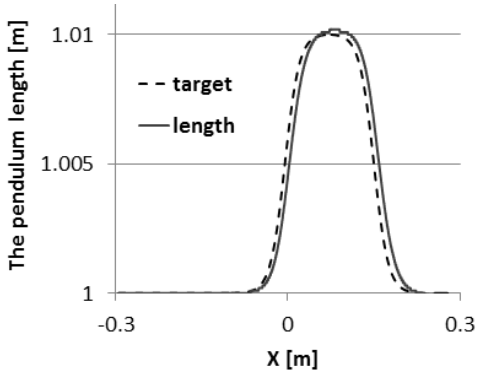

Fig. 8. The value of target trajectory and the length of the inverted pendulum when $\alpha = 80$, $\beta_1 = -0.005$ and $\beta_2 = 0.15$

Fig. 9 shows simulation results. Fig. 9 (a), (c) and (e) show the values of ΔE when we changed the value of β_1 from -0.10 to 0.05 with some sets of α and β_2. We obtained the following equation from the dynamic equation eq. (9) to analyze these results.

$$l\ddot{\theta} = -2\dot{l}\dot{\theta} + gsin\theta \tag{11}$$

From this equation, expanding the length of pendulum has an effect of decelerating the angular velocity. In addition, shortening the length of pendulum has an effect of accelerating the angular velocity. Therefore, the first term of the right side of eq. (11) has the effect of excitation. The first term of right side has a non-zero value while the length of the pendulum is varied. From Fig. 5-7, the interval between extending and shortening the length of the pendulum became wide when α was small or the distance from β_1 to β_2 was long. From Fig. 9, the inclement of mechanical energy ΔE became large when α was small or β_2 was large. From these results, proposed target trajectory has the similar characteristics of the parametrically excited inverted pendulum.

From Fig. 9 (c) and (e), the increment of mechanical energy peaked around $\beta_1 = 0$. These results match the theory of the optimal trajectory. Fig. 8 shows the target trajectory and the length of the inverted pendulum when $\beta_1 = -0.005$, $\beta_2 = 0.15$ and $\alpha = 80$. From this figure, the inverted pendulum accurately followed the target trajectory. However, from Fig. 9 (a), the increment of mechanical energy ΔE peaked when

TABLE I
PHYSICAL PARAMETERS USED IN THE SIMULATION

parameter	value	unit	parameter	value	unit
m	1.0	[Kg]	A	0.01	[m]
l_0	1.00	[m]	α	40 - 80	[-]
θ_0	-0.30	[rad]	β_1	-0.10 $\sim$ 0.05	[m]
			β_2	0.10 $\sim$ 0.15	[m]

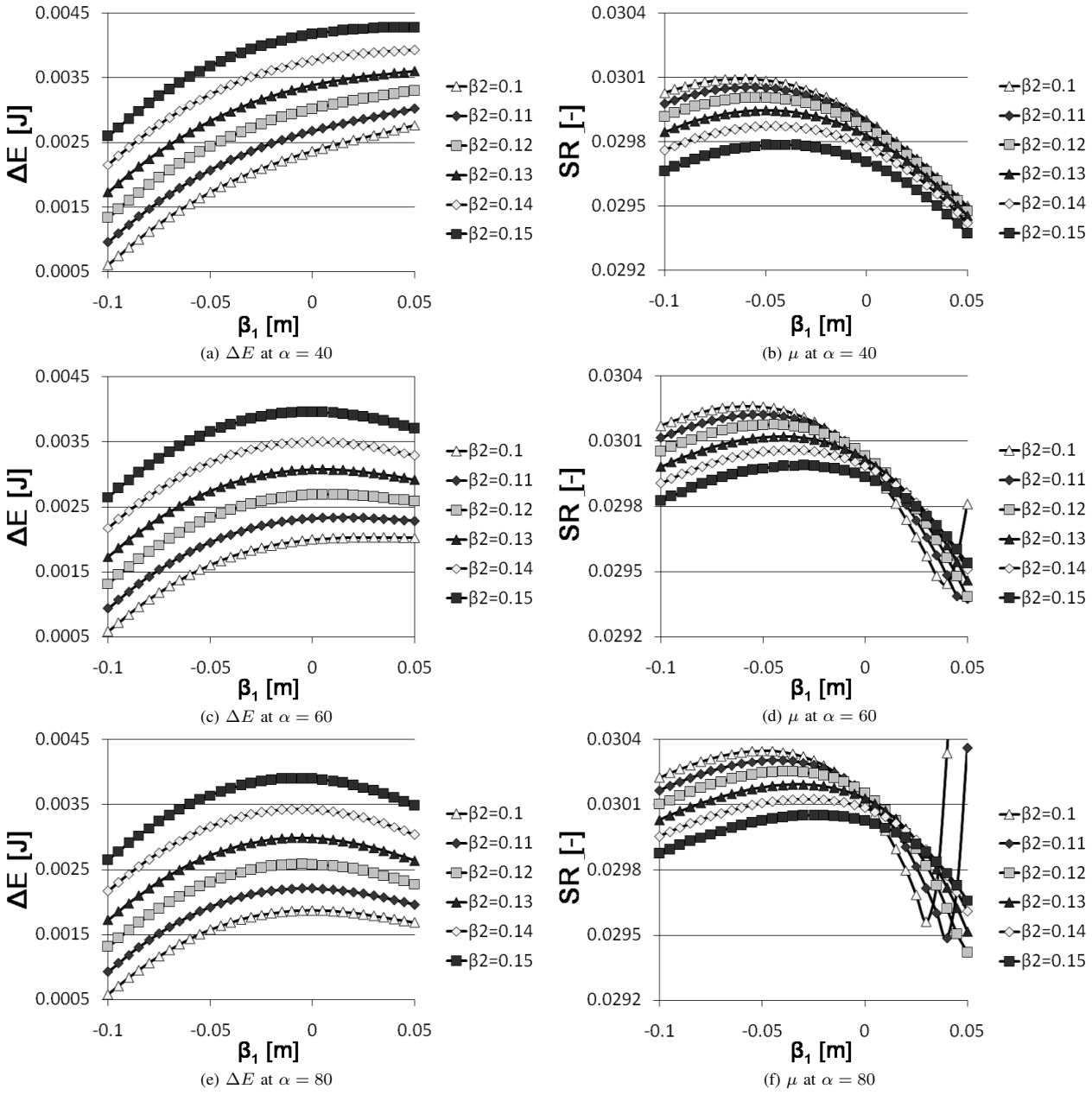

(a) ΔE at $\alpha = 40$ (b) μ at $\alpha = 40$

(c) ΔE at $\alpha = 60$ (d) μ at $\alpha = 60$

(e) ΔE at $\alpha = 80$ (f) μ at $\alpha = 80$

Fig. 9. Mechanical energy inclement ΔE and the specific resistance μ with respect to β_1 with six values of β_2

β_1 was larger than zero. When α was small or the distance from β_1 to β_2 was long, $\hat{A}$ that was described by eq. (7) had large value. Therefore, the actual rising position became smaller than β_1 and the actual falling position became larger than β_2. It is suggested that this effect of the normalization contributed to the increment of mechanical energy.

Fig. 9 (b), (d) and (f) show the values of μ when we change the value of β_1 from -0.10 to 0.05 with some sets of α and β_2. The shorter the distance from β_1 to β_2 became, the smaller μ became. However, from Fig. 9 (d) and (f), energy efficiency became greatly worse because the length of pendulum rapidly expanded and shortened when α became large and the distance from β_1 to β_2 became very short. In addition, the inclement of β_2 improved the energy efficiency. Therefore, it is suggested that gentle expanding and shortening the length of pendulum contributes to the inclement of mechanical energy and energy efficiency.

IV. Walking simulations

In this section, we verify the effect of our target trajectory for bipedal walking via numerical simulations.

The biped robot was described in previous section. This robot has only knee actuation. Therefore, we applied our proposed target trajectory to the relative knee angle $\theta_K =$

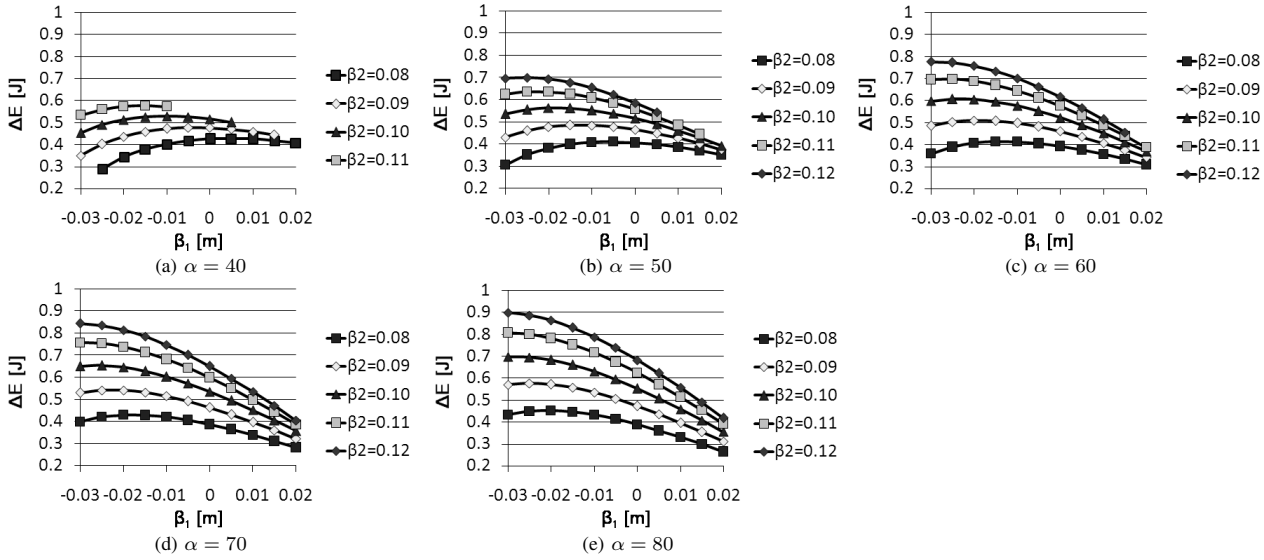

(a) $\alpha = 40$ (b) $\alpha = 50$ (c) $\alpha = 60$

(d) $\alpha = 70$ (e) $\alpha = 80$

Fig. 10. Mechanical energy incrementation ΔE with respect to β_1 with five values of β_2

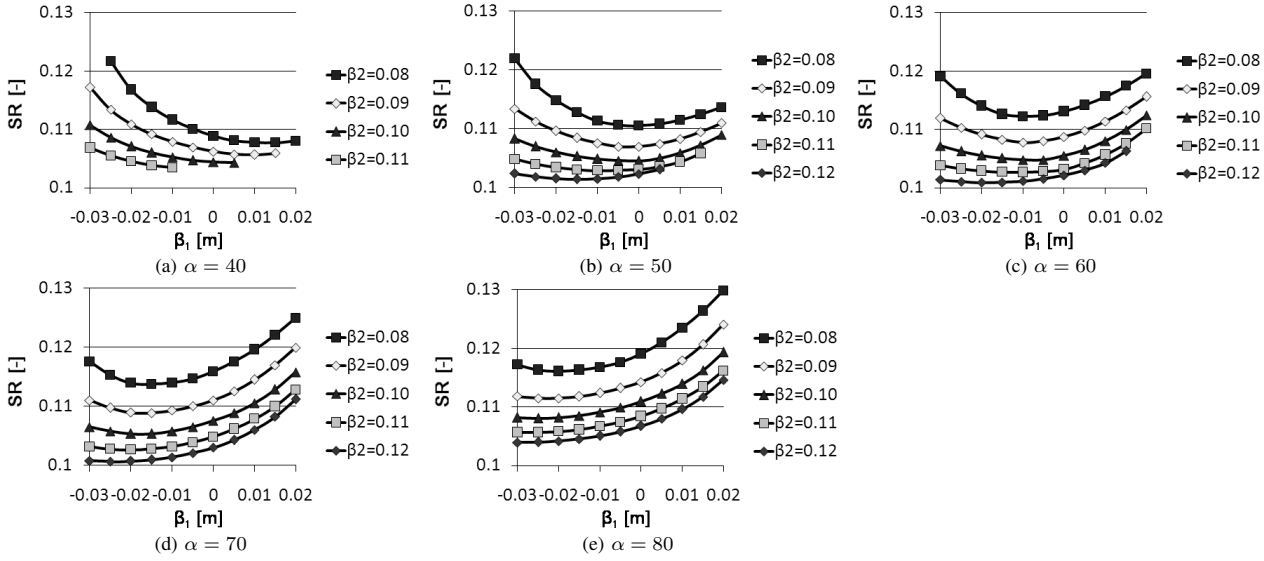

(a) $\alpha = 40$ (b) $\alpha = 50$ (c) $\alpha = 60$

(d) $\alpha = 70$ (e) $\alpha = 80$

Fig. 11. The specific resistance μ with respect to β_1 with five values of β_2

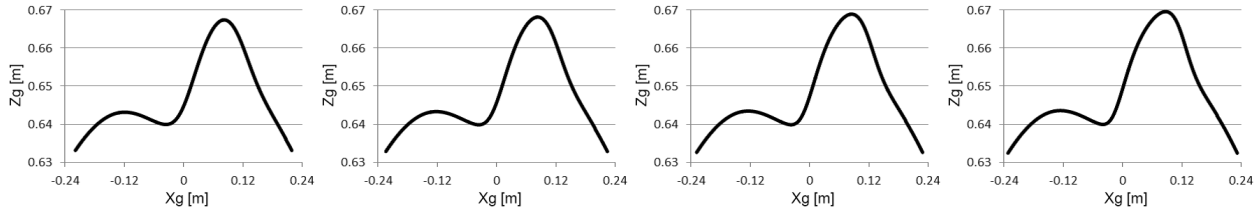

(a) $\alpha = 50$ and $\beta_1 = -0.01$ (b) $\alpha = 60$ and $\beta_1 = -0.015$ (c) $\alpha = 70$ and $\beta_1 = -0.025$ (d) $\alpha = 80$ and $\beta_1 = -0.03$

Fig. 12. Center of mass trajectory corresponding to four parameter sets when $\beta_2 = 0.12$

$-(\theta_2 - \theta_3)$. The angular trajectory of knee joint is represented by

$$\theta_{Kd}(x) = \frac{\hat{A}}{1 + e^{-\alpha(x-\beta_1)}} \times \frac{1}{1 + e^{\alpha(x-\beta_2)}}. \qquad (12)$$

We evaluated two walking performances of this robot when the parameters α, β_1 and β_2 were varied. Two walking performances are the restored energy and the specific resistance during one step. Physical parameters of this robot are listed in Table II.

Fig. 10-11 show simulation results. Fig. 10 shows the values of ΔE when we changed the value of β_1 from -0.03 to 0.02 with some sets of α and β_2. From Fig. 10, the increment of

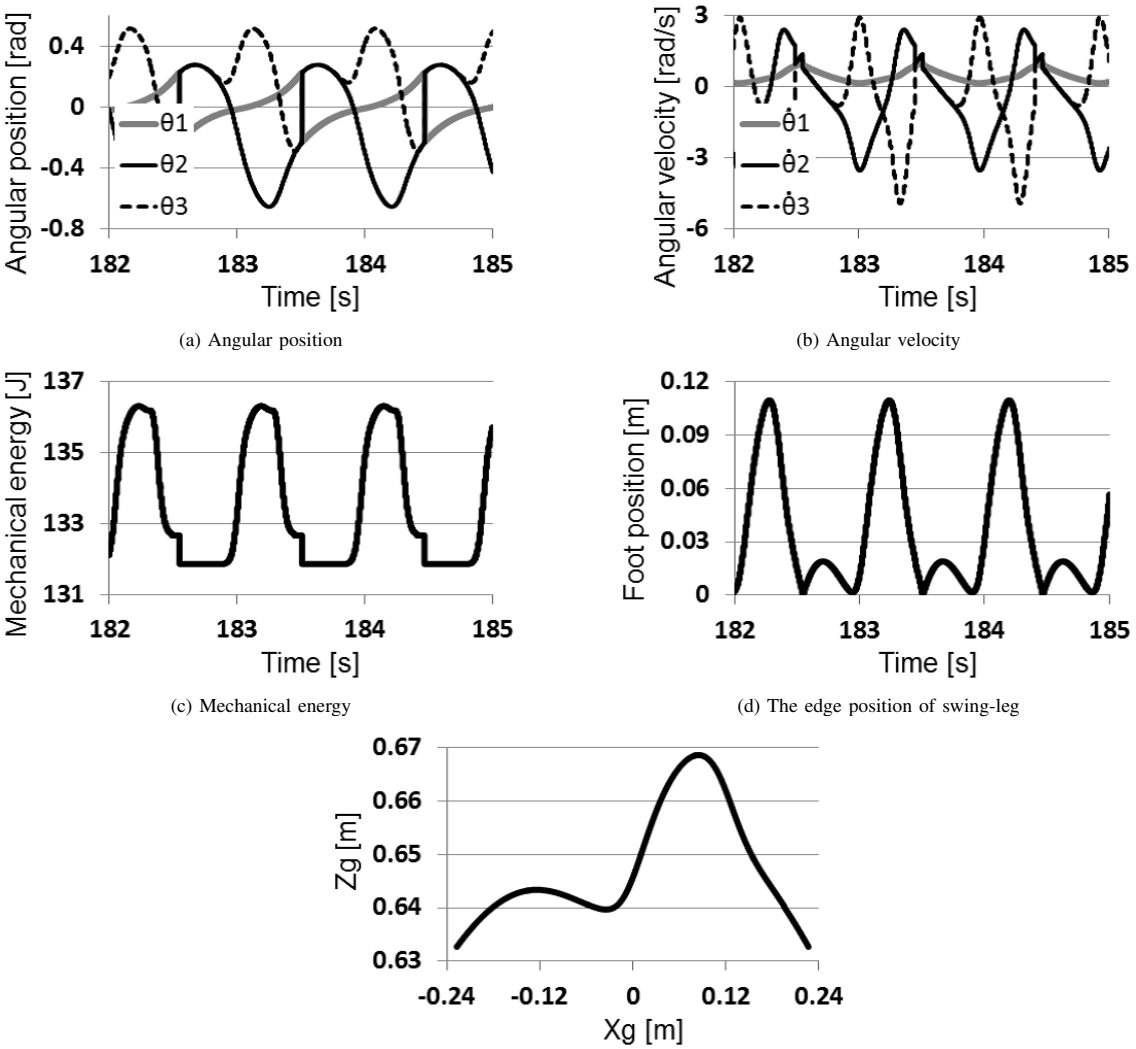

(a) Angular position

(b) Angular velocity

(c) Mechanical energy

(d) The edge position of swing-leg

(e) Center of mass

Fig. 13. Results of bipedal walking when $\alpha = 68$, $\beta_1 = -0.02$ and $\beta_2 = 0.12$

mechanical energy peaked around $\beta_1 = 0$. These results match the theory of the optimal trajectory and simulation results of an inverted pendulum. The larger the values of α and β_2 became, the greater the restored energy became.

Fig. 11 shows the values of μ when we changed the value of β_1 from -0.03 to 0.02 with some sets of α and β_2. From Fig. 11, the specific resistance μ reached a minimum value around $\beta_1 = 0$. The larger the values of β_2 became, the smaller the specific resistance μ became. In addition, there was the value of α that made the energy efficiency the highest. When $\alpha = 68$, $\beta_1 = -0.02$ and $\beta_2 = 0.12$, the most efficient walking was achieved. Fig. 12 shows the trajectory of mass center with respect to four parameter sets. The trajectories were similar to each other and these mass centers move higher around $X_g = 0$. Therefore, it is suggested that there is the optimal trajectory of mass center for efficient walking. In addition, the robot achieved stable walking with many parameter sets when α was large. Therefore, we need to select the suitable parameters that improve energy efficiency or the stability of walking.

TABLE II
PHYSICAL PARAMETERS USED IN THE WALKING SIMULATION

parameter	value	unit	parameter	value	unit
L	1.0	[m]	R	0.4	[m]
b_1	0.35	[m]	m_1	5.0	[Kg]
L_2	0.5	[m]	m_2	1.0	[Kg]
L_3	0.5	[m]	m_3	4.0	[Kg]
a_2	0.25	[m]	m_H	8.0	[Kg]
a_3	0.25	[m]	A	1.0	[rad]

Fig. 13 shows the results of walking states. From Fig. 13 (d), it is ovserved that the foot clearance problem was avoided. The foot clearance problem is the phenomenon that the foot of the robot passes through the ground during the step. Fig. 14 shows the stable gait conditions during one step.

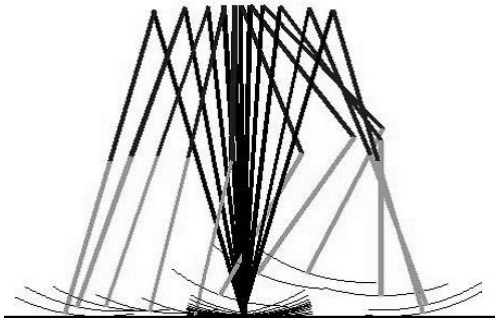

Fig. 14. Stick figures of walking when $\alpha = 68$, $\beta_1 = -0.02$ and $\beta_2 = 0.12$

V. Conclusion

In this paper, we proposed a new target trajectory that is described as a function of spatial position for efficient parametrically excited walking with the knee joint actuation. Proposed target trajectory is based on a position in the walking direction. Therefore, the knee joint is bent at the desired interval when the walking speed or walking stride is varied. Firstly, we verified that our proposed target trajectory had the characteristics of a parametrically excited inverted pendulum via numerical simulations. Secondly, we applied this target trajectory to the knee joint of a bipedal robot. Then, we verified the validity of our proposed target trajectory for bipedal walking. As a result, we found that there was an optimal parameter set for efficient parametrically excited walking with knee joint actuation.

References

[1] T. McGeer, "Passive Dynamic Walking," *Int.J. of Robotics Research*, Vol.57, No.2, pp.62-82, 1990.
[2] A. Goswami, B. Espiau and A. Keramane, "Limit cycles in a passive compass gait biped and passivity-mimicking control laws," *J. of Autonomous Robots*, Vol.4, No. 3, pp.273-286 1997.
[3] F. Asano, M. Yamakita and K. Furuta, "Virtual passive dynamic walking and energy-based control laws," *IEEE/RSJ International Conference on Intelligent Robotics and Systems*, 2000.
[4] F. Asano and Z. W. Luo, "The effect of semicircular feet on energy dissipation by heel-strike in dynamic biped locomotion," *IEEE International Conferance on Robotics and Automation*, 2007.
[5] F. Asano and Z. W. Luo, "Efficient dynamic bipedal walking using effects of semicircular feet," *Robotica*, Vol 29, pp.351-365, 2011.
[6] F. Asano, Z. W. Luo and S. Hyon, "Parametric excitation mechanisms for dynamic bipedal walking," *IEEE International Conference on Robotics and Automation*, 2005.
[7] F. Asano, T. Hayashi, Z. W. Luo, S. Hirano and A. Kato, "Parametric excitation approaches to efficient bipedal walking," *IEEE/RSJ International Conference on Intelligent Robots and Systems*, 2007.
[8] F. Asano and Z. W. Luo, "Energy-efficient and high-speed dynamic biped locomotion based on principle of parametric excitation," *IEEE Transaction on Robotics*. Vol.24, No.6, pp.1289-1301, 2008.
[9] Y. Harata, F. Asano, K. Taji and Y. Uno, "Biped gait generation based on parametric excitation by knee-joint actuation," *IEEE/RSJ International Conference on Intelligent Robots and Systems*, 2007.
[10] Y. Harata, F. Asano, K. Taji and Y. Uno, "Efficient parametric excitation walking with delayed feedback control," *IEEE/RSJ International Conference on Intelligent Robots and Systems*, 2009.
[11] Y. Harata, F. Asano, Z. W. Luo, K. Taji and Y. Uno, "Biped gait generation based on parametric excitation by knee-joint actuation," *Robotica*, Vol. 27, pp.1063-1073, 2009.
[12] T. Honjo, A.Nagano and Z. W. Luo, "Parametric excitation of a biped robot as an inverted pendulum," *IEEE/RSJ International Conference on Intelligent Robots and Systems*, 2008.
[13] Y. Banno, Y. Harata, K. Taji and Y. Uno, "Optimal trajectory design for parametric excitation walking," *IEEE/RSJ International Conference on Intelligent Robots and Systems*, 2009.
[14] Y. Harata, Y. Banno and K. Taji, "Parametric excitation based bipedal walking: Control method and optimization," *Numerical Algebra, Control and Optimization*, Vol.1, No.1, pp.171-190, 2011.

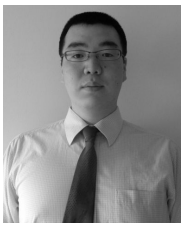

Toyoyuki Honjo received his bachelor's and master's degree in engineering from Kobe University, Kobe, Japan, in 2008 and 2009, respectively. Currently, he is a doctorial course student at Kobe University. His research interest includes biped locomotion, dynamical system and human walking. He is a student member of the Robotics Society of Japan (RSJ) and IEEE Robotics and Automation society.

Takeshi Hayashi received his master's degree from the Aichi Institute of Technology in 2008. He continued his graduate work at Kobe University and obtained a doctor's degree in 2011. Now he works as a post-doctoral researcher at National institute of advanced industrial science and technology. His research interest includes robotics and bio-mechanics.

Akinori Nagano received his master's degree from the University Tokyo in 1998. He continued his graduate work at Arizona State University and obtained a doctor's degree in 2001. He worked as a post-doctoral researcher at Boston University, Harvard Medical School and RIKEN before obtaining a lecturer's position at the University of Aberdeen, UK. He moved to Kobe University as an Associate Professor in September 2007. His research interest includes biomechanics, motor control and rehabilitation engineering. He has authored over 40 research articles in international and domestic journals.

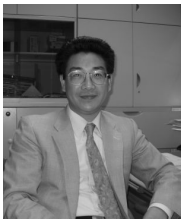

Zhi-Wei Luo received the B.E. degree in engineering from Huazhong University of Science and Technology, Wuhan, China, in 1984 and M.Eng. and Dr. Eng. degrees in information engineering from Nagoya University, Nagoya, Japan, in 1991 and 1992, respectively. From 1984 to 1986, he was a teacher at Suzhou University, China. From 1986 to 1988, he was a Visiting Scholar with the Aichi Institute of Technology, Japan. From 1992 to 1994, he was an Assistant Professor with Toyohashi University of Technology, Japan. From 1994 to 1998, he was a Frontier Researcher with the Bio-Mimetic Control Research Center, Institute of Physical and Chemical Research (RIKEN), where since 2001, he has been the Laboratory Head of the Environment Adaptive Robotic Systems Laboratory, where he has led the development of a human interactive robot known as RI-MAN. From 1999 to 2001, he was an Associate Professor at Yamagata University, Yamagata. He is currently a Professor at Kobe University, Kobe, Japan. His current research interests include robotics, system control theory and biomimetics. Prof. Luo is a member of the Robotics Society of Japan (RSJ) and the Society of Instrument and Control Engineers (SICE). He is an Associate Editor of IEEE Transactions on Robotics.